

Novel features of diffraction at the LHC

V. A. Petrov, A. V. Prokudin, S. M. Troshin, N. E. Tyurin

*Institute for High Energy Physics,
Protvino, Moscow Region, 142280, Russia*

Abstract

Interest and problems in the studies of diffraction at LHC are highlighted. Predictions for the global characteristics of proton-proton interactions at the LHC energy are given. Potential discoveries of the antishadow scattering mode which is allowed in principle by unitarity and diffractive scattering conjugated with high- E_T jets are discussed.

Introduction

During recent years CERN, DESY and FNAL have been producing interesting results on diffractive production in hadron and deep-inelastic processes [1]. Discovery of hard diffraction at CERN $S\bar{p}pS$ [2] and diffractive events in the deep-inelastic scattering at HERA [3, 4] were among the most surprising results obtained recently. Significant fraction of high- t events among the diffractive events in deep-inelastic scattering and in hadron-hadron interactions were also observed at HERA [5] and Tevatron [6] respectively. These experimental findings have renewed interest in the experimental and theoretical studies of the diffractive production processes.

There are many unsolved problems in soft and hard hadronic physics which should be studied at the highest possible energies at the LHC and their importance should not be overshadowed by the expectations for the new particles in this newly opening energy range. We consider several such problems in some details in this note.

First of all one deals with genuinely **strong interactions**, which are not corrections to the free or lowest-order dynamics (this is the case of purely hard processes where perturbative QCD is able (with some serious reservations, though) to make predictions and descriptions). In this regime it is possible that the interaction will enter the new scattering mode – antishadow scattering which is in principle allowed by unitarity and may be realized in the region of the strong coupling [7]. However, it is not necessarily realized in nature and only the experimental studies can provide the crucial answer.

It is useful to estimate spatial extension of the diffractive processes. From the Heisenberg uncertainty relations one gets, e. g. for elastic scattering,

$$\begin{aligned}
 \Delta x_i \Delta p_i &\geq 1, \quad i = \parallel, \perp \\
 (\Delta p_{\parallel})^2 &= (\langle t^2 \rangle - \langle t \rangle^2) / 4p^2, \\
 4p^2 &= s - 4m^2 \\
 (\Delta p_{\perp})^2 &= -\langle t \rangle + \langle t \rangle^2 / 4p^2,
 \end{aligned} \tag{1}$$

and at high energies

$$\begin{aligned}
 \Delta x_{\parallel}^* &\geq \sqrt{s} / \sqrt{\langle t^2 \rangle - \langle t \rangle^2} \\
 \Delta x_{\perp} &\geq 1 / \sqrt{\langle -t \rangle},
 \end{aligned} \tag{2}$$

where Δx_{\parallel}^* and Δx_{\perp} are longitudinal and transverse coordinate uncertainties, correspondingly in the c. m. s., \sqrt{s} is the total c. m. s. energy. It should be noted that our formulas refer to final state momenta which are stochastic due to fluctuations (quantum-mechanical) in the scattering angle and our definition of $(\Delta p)^2$ looks

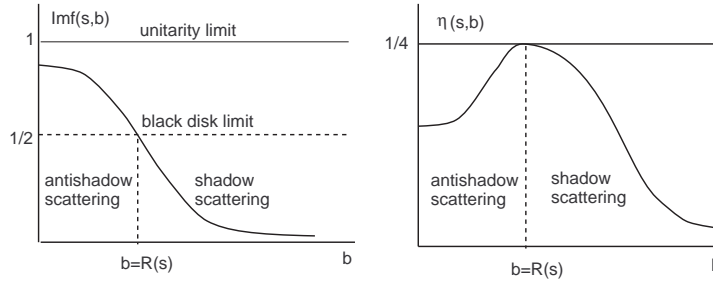


Figure 1: Shadow and antishadow scattering regions

like the following: $\langle p_{\parallel} \rangle = p \langle \cos(\theta) \rangle$, $\langle p_{\parallel}^2 \rangle = p^2 \langle \cos^2(\theta) \rangle$ and then we take as usual

$$(\Delta p_{\parallel})^2 = p^2 (\langle \cos^2 \theta \rangle - \langle \cos \theta \rangle^2);$$

similarly for Δp_{\perp} , but there we know due to azimuthal symmetry that $\langle \vec{p}_{\perp} \rangle = 0$.

In diffractive processes average momentum transfers $\langle -t \rangle$, $\langle t^2 \rangle$ depend only weakly on s so we will deal with **large distances** at LHC. For instance

$$\Delta x_{\parallel}^* > 40000 \text{ fm} !$$

At such long distances description of the high-energy collisions in terms of individual partons — quarks and gluons ceases to be adequate. We enter a new territory where confinement dynamics is overwhelming and some (gluon) field configurations become relevant degrees of freedom. In other words diffractive high-energy scattering deals with undulatory aspects of the QCD dynamics.

This field is one of the greatest challenges to both theoretical and experimental high-energy physics communities.

1 Antishadow Scattering at LHC

Unitarity of the scattering matrix $SS^+ = 1$ implies the existence at high energies $s > s_0$ of the new scattering mode – antishadow one. It has been described in some detail (cf. [8] and references therein) and the most important feature of this mode is the self-damping of the contribution from the inelastic channels. We argue here that the antishadow scattering mode could be definitely revealed at the LHC energy and provide numerical estimations based on the U -matrix unitarization method [9]. In the impact parameter representation the unitarity relation written for the elastic scattering amplitude $f(s, b)$ at high energies has the form

$$\text{Im}f(s, b) = |f(s, b)|^2 + \eta(s, b) \quad (3)$$

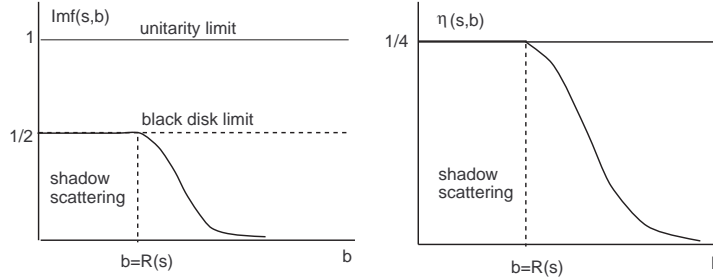


Figure 2: Shadow scattering mode

where the inelastic overlap function $\eta(s, b)$ is the sum of all inelastic channel contributions. Unitarity equation has two solutions for the case of pure imaginary amplitude:

$$f(s, b) = \frac{i}{2} [1 \pm \sqrt{1 - 4\eta(s, b)}]. \quad (4)$$

Eikonal unitarization

$$f(s, b) = \frac{e^{2i\delta(s,b)} - 1}{2i} \quad (5)$$

with pure imaginary eikonal ($\delta = i\Omega/2$) corresponds to the choice of the one particular solution of the unitarity equation with sign minus.

In the U -matrix approach the form of the elastic scattering amplitude in the impact parameter representation is the following:

$$f(s, b) = \frac{U(s, b)}{1 - iU(s, b)}. \quad (6)$$

$U(s, b)$ is the generalized reaction matrix, which is considered as an input dynamical quantity similar to eikonal function.

Inelastic overlap function is connected with $U(s, b)$ by the relation

$$\eta(s, b) = \frac{ImU(s, b)}{|1 - iU(s, b)|^2}. \quad (7)$$

It is worth noting that the shadow scattering mode is considered usually as the only possible one. But the two solutions of the unitarity equation have an equal meaning and the antishadow scattering mode should not be excluded.

Appearance of the antishadow scattering mode is completely consistent with the basic idea that the particle production is the driving force for elastic scattering. Let us consider the transition to the antishadow scattering mode [7].

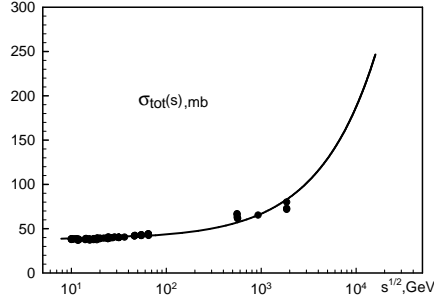


Figure 3: Total cross-section of pp -interactions, experimental data from [12]

With conventional parameterizations of the U -matrix the inelastic overlap function increases with energies at modest values of s . It reaches its maximum value $\eta(s, b = 0) = 1/4$ at some energy $s = s_0$ and beyond this energy the antishadow scattering mode appears at small values of b . The region of energies and impact parameters corresponding to the antishadow scattering mode is determined by the conditions $Imf(s, b) > 1/2$ and $\eta(s, b) < 1/4$. The quantitative analysis of the experimental data [10] gives the threshold value of energy: $\sqrt{s_0} \simeq 2$ TeV. This value is confirmed by the recent model considerations [11].

Thus, the function $\eta(s, b)$ becomes peripheral when energy is increasing. At such energies the inelastic overlap function reaches its maximum value at $b = R(s)$ where $R(s)$ is the interaction radius. So, beyond the transition threshold there are two regions in impact parameter space: the central region of antishadow scattering at $b < R(s)$ and the peripheral region of shadow scattering at $b > R(s)$. The impact parameter dependence of the amplitude $f(s, b)$ and inelastic channel contribution $\eta(s, b)$ at $s > s_0$ are represented on Fig. 1.

The region of LHC energies is the one where antishadow scattering mode is to be presented. This mode can be revealed directly measuring $\sigma_{el}(s)$ and $\sigma_{tot}(s)$ and not only through the analysis in impact parameter representation.

Note that the impact parameter behavior of the amplitude and the inelastic overlap function have the form depicted on the Fig. 2 in case when the only shadow scattering is realized at the LHC energies.

For the LHC energy $\sqrt{s} = 14$ TeV the model based on the U -matrix form of unitarization provides (Fig. 3)

$$\sigma_{tot} \simeq 230 \text{ mb} \quad (8)$$

and

$$\sigma_{el}/\sigma_{tot} \simeq 0.67. \quad (9)$$

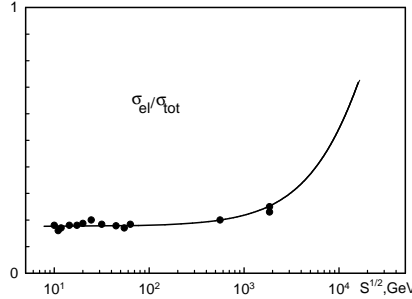


Figure 4: Ratio of elastic to total cross-section of pp -interactions, experimental data from [12]

Thus, the antishadow scattering mode could be discovered at LHC by measuring σ_{el}/σ_{tot} ratio which is greater than the black disc value $1/2$ (Fig. 4).

However, the LHC energy is not in the asymptotic region yet, the asymptotical behavior

$$\sigma_{tot,el} \propto \ln^2 s, \quad \sigma_{inel} \propto \ln s \quad (10)$$

is expected at $\sqrt{s} > 100 \text{ TeV}$.

The above predicted values for the global characteristics of pp – interactions at LHC differ from the most common predictions of the other models. First of all total cross-section is predicted to be twice as much of the common predictions in the range 95-120 mb [13] and it even overshoots the existing cosmic ray data. However, extracting proton-proton cross sections from cosmic ray experiments is model dependent and far from straightforward (see, e.g. [14] and references therein). It should be noted here that the large value of the total cross-section is due to the elastic scattering while the value of inelastic cross-section is about 80 mb and close to the common predictions. Therefore, the large value of the total cross-section does not imply the large background.

2 Inelastic Diffraction at LHC

Similarity between elastic and inelastic diffraction in the t -channel approach suggests that the latter one would have similar to elastic scattering behavior of the differential cross-section. However, it cannot be taken for granted and e.g. transverse momentum distribution of diffractive events in the deep-inelastic scattering at HERA shows a power-like behavior without apparent dips [15]. Similar behavior was observed also in the hadronic diffraction dissociation process at CERN

[2] where also no dip and bump structure was observed. Angular dependence of diffraction dissociation together with the measurements of the differential cross-section in elastic scattering would allow to determine the geometrical properties of elastic and inelastic diffraction, their similar and distinctive features and origin.

It is interesting to note that at large values of the missing mass M^2 the normalized differential cross-section $\frac{1}{\sigma_0} \frac{d\sigma_D}{dt dM^2}$ (σ_0 is the value of cross-section at $t = 0$) will exhibit scaling behavior [16]

$$\frac{1}{\sigma_0} \frac{d\sigma_D}{dt dM^2} = f(-t/M^2), \quad (11)$$

and explicit form of the function $f(-t/M^2)$ is the following

$$f(-t/M^2) = (1 - 4\xi^2 t/M^2)^{-3}. \quad (12)$$

This dependence is depicted on Fig. 5.

The above scaling has been obtained in the model approach, however it might have a more general meaning. Conventional diffractive inelastic scattering predictions on the basis of the triple-reggeon phenomenology do not exhibit t/M^2 -scaling.

The angular structure of diffraction dissociation processes given by Eq. (11) takes place at high energies where while at moderate and low energies dip-bump structure can be presented [16]. Thus at low energies the situation is similar to the elastic scattering, i.e. diffraction cone and possible dip-bump structure should be present in the region of small values of t and behavior of the differential cross-section will be rather complicated and incorporates diffraction cone, Orear type (exponential behavior with $\sqrt{-t}$) and power-like dependencies.

At the LHC energy the diffractive events with the masses as large as 3 TeV could be studied. It would be interesting to check this prediction at the LHC where the scaling and simple power-like behavior of diffraction dissociation differential cross-section should be observed. Observation of such behavior would confirm the diffraction mechanism based on excitation of the complex hadronlike object - constituent quark. This mechanism can in principle explain angular structure of diffraction in the deep - inelastic scattering at HERA where smooth angular dependence on the thrust transverse momentum was observed [15]. If it is the case, then diffraction in DIS at lower energies should manifest typical soft diffractive behavior with exponential peak at small t as it does in hadronic reactions.

3 Hard and Soft Diffraction Interplay at LHC

In principle measurements of the global characteristics, like σ_{tot} , σ_{el} , $\sigma_{D(D)}$, $d\sigma/dt$ etc. may be considered as a source of information on the size and shape of the interaction region. To some extent this can be assimilated to the famous ‘‘inverse

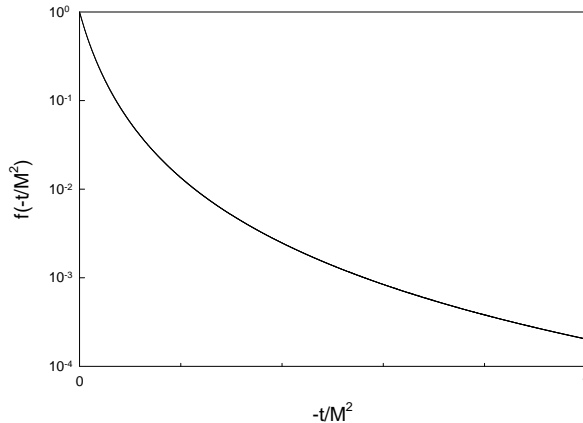


Figure 5: Scaling behavior of the normalized differential cross-section $\frac{1}{\sigma_0} \frac{d\sigma}{dt dM^2}$.

scattering problem” in potential scattering, where the problem is, roughly, to extract an unknown potential from the “data” (phase shifts).

This stage of study is, in principle, model independent. Only after getting an information on the interaction region can one ask if, say, QCD is able to describe and explain it.

When generic diffractive processes proceed it may happen that due to vacuum fluctuations some short-time perturbation will take place, resulting in appearing of hard scattered partons which we percept as hadronic jets. Such a perturbation may quite strongly influence the interaction region which can result in a spectacular change of the normal diffractive pattern.

As an example one can consider the process (Fig. 6)

$$p + p \rightarrow p + \text{jet} + \text{jet} + p,$$

where two jets are safely separated from “diffractive” protons by rapidity gaps.

The study of a change of a diffractive pattern may be realized as a joint on-line measurement by CMS (jets and rapidity gaps) and TOTEM (“diffractive protons” at Roman Pots) [17]. The dependence of a symmetric ($t_1 = t_2 = t$) t -distribution at two values of E_T is pictured at Fig. 7. The squared sub-energies $s_{1,2}$ are supposed to be in the asymptotical region.

4 Conclusion

The studies of soft interactions at the LHC energies can lead to the discoveries of fundamental importance. The evolution of hadron scattering with rising energy

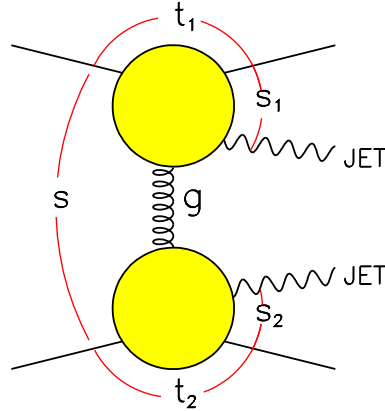


Figure 6: Schematic representation of the process $p + p \rightarrow p + \text{jet} + \text{jet} + p$.

can be described as transition from the grey to black disc and eventually to black ring with the antishadow scattering mode in the center. It is worth noting that the **appearance of the antishadow scattering mode** at the LHC energy implies a somewhat unusual scattering picture. At high energies the proton should be realized as a loosely bounded composite system and it appears that this system has a high probability to reinstate itself only in the central collisions where all of its parts participate in the coherent interactions. Therefore the central collisions are responsible for elastic processes while the peripheral ones where only few parts of weakly bounded protons are involved result in the production of the secondary particles. This leads to the peripheral impact parameter profile of the inelastic overlap function.

We have to emphasize once again that from the space–time point of view high–energy diffractive processes reveal **larger and larger distances and times** which is a real **terra incognita** “filled” with still unknown gluon field configurations evidently responsible for **confinement dynamics**.

There could be envisaged various experimental configurations at the LHC; e.g. soft diffraction goes well to the interest of the TOTEM experiment, while hard diffractive final states can be measured by CMS detector and possible **correlations between the features of the soft and hard diffractive processes** can be obtained using combined measurements of TOTEM and CMS [18].

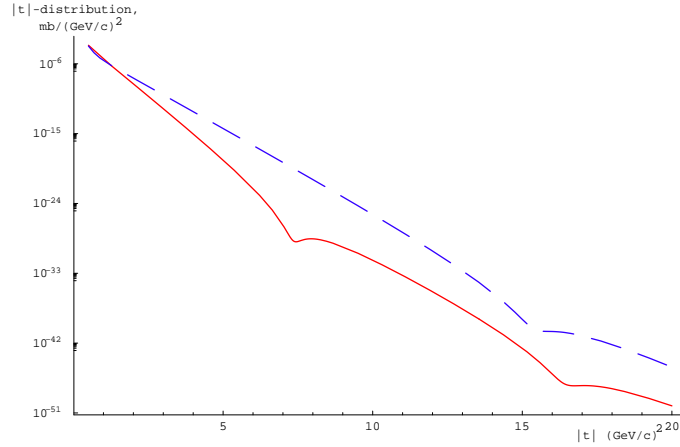


Figure 7: $s_{1,2} \simeq \sqrt{s}E_t$, $Q^2 \simeq 2E_t^2$, solid line corresponds to $E_t = 10$ GeV, dashed line corresponds to $E_t = 100$ GeV; $\sqrt{s} = 14$ TeV.

References

- [1] D. M. Jansen, M. Albrow and R. Brugnera, hep-ph/9905537.
- [2] R. Bonino et al., Phys. Lett. B 211 (1988) 239; A. Brandt et al., Nucl. Phys. B 514 (1998) 3.
- [3] T. Ahmed et al., Phys. Lett. B 348 (1995) 681.
- [4] M. Derrick et al., Z. Phys. C. 68 (1995) 569.
- [5] C. Adloff et al., Z. Phys. C. 76 (1997) 613.
- [6] L. Alvero et al., Phys. Rev. D 59 (1999) 074022.
- [7] S. M. Troshin and N. E. Tyurin, Phys. Lett. **B 316** (1993) 175.
- [8] S. M. Troshin and N. E. Tyurin, Phys. Part. Nucl. 30 (1999) 550.
- [9] A. A. Logunov, V. I. Savrin, N. E. Tyurin and O. A. Khrustalev, Teor. Mat. Fiz. **6** (1971) 157;
- [10] P. M. Nadolsky, S. M. Troshin and N. E. Tyurin, Z. Phys. C **69** (1995) 131 .
- [11] P. Desgrolard , L. Jenkovszky, B. Struminsky, Eur. Phys. J. C **11** (1999) 144;
P. Desgrolard, hep-ph/0106043.
- [12] The computer readable files available at <http://pdg.lbl.gov>.
- [13] J. Velasco , J. Perez-Peraza, A. Gallegos-Cruz, M. Alvarez-Madrigal, A. Faus-Golfe, A. Sanchez-Hertz, hep-ph/9910484

- [14] M. M. Block, F. Halzen and T. Stanev, hep-ph/9908222.
- [15] C. Adloff et al., Eur. Phys. J. 1998 V. C10, 443 .
- [16] S. M. Troshin and N. E. Tyurin, hep-ph/0008274.
- [17] The TOTEM Collaboration, Technical Proposal CERN/LHCC 99-7, LHCC/P5, 1999.
- [18] V. A. Petrov, talk given at the International Symposium “ LHC Physics and Detectors”, Dubna, 28-30 June 2000.